Available online at www.sciencedirect.com

SciVerse ScienceDirect

Ceramics International 38 (2012) 1951–1957

CERAMICS INTERNATIONAL

www.elsevier.com/locate/ceramint

Synthesis, structural and magnetic characterization of nanocrystalline $CuFe_2O_4$ as obtained by a combined method reactive milling, heat treatment and ball milling

T.F. Marinca [a,b], I. Chicinaş [a,*], O. Isnard [b]

[a] Materials Sciences and Technology Department, Technical University of Cluj-Napoca, 103-105 Muncii Avenue, 400641 Cluj-Napoca, Romania
[b] Institut Néel, CNRS and Université Joseph Fourier, 25 rue des Martyrs, 38042 Grenoble, France

Received 30 August 2011; accepted 11 October 2011
Available online 17 October 2011

Abstract

Nanocrystalline copper ferrite has been synthesized using a combined method which involves reactive milling, heat treatment and mechanical milling. After 4 h of reactive milling a solid solution between the starting oxides (CuO and α-Fe_2O_3) and a spinel phase is obtained. Increasing the milling time leads to a decomposition of those phases. After a heat treatment of the 30 h milled sample a single spinel $CuFe_2O_4$ phase is obtained. By mechanical milling the crystallite size of the copper ferrite is reduced down to 9 nm after 1 h of milling. For the $CuFe_2O_4$ samples milled between 2 and 4 h a decomposition of this phase is remarked and α-Fe_2O_3 is formed during milling. The spontaneous magnetization of the spinel decreases with increasing the milling time as results of the partial redistribution of the cations in the spinel and of spin canted effect. The magnetization of the milled samples does not saturate due to the presence of very fine ferrite particles which are superparamagnetic.

Keywords: A. Milling; B. Grain size; C. Magnetic properties; D. Ferrites

1. Introduction

Soft magnetic spinel ferrites ($MeFe_2O_4$, where Me is a bivalent metallic ion or a combination of these) are a large class of magnetic materials and one of the most studied magnetic system. Their magnetic and electrical properties recommended them for many technical and industrial applications [1–5]. The spinel structure characteristic for the soft magnetic ferrites present two type of crystallographic sites for the metallic cations, Fe^{3+} and Me^{2+}: tetrahedral sites (A sites) and octahedral sites (B sites). In normal spinel structures the A sites are occupied by the Me^{2+} cations and the B sites are occupied by Fe^{3+}. In inverse spinel structure, the Me^{2+} cations are in B sites and the Fe^{3+} are equally distributed between A and B sites. There are also ferrites which present partially inverse spinel structure [6]. Among the soft ferrites, the copper ferrite ($CuFe_2O_4$) is one of the most interesting [4,7–10]. Typically, the structure of copper ferrite is an inverse spinel (Cu^{2+} being located in tetrahedral sites). The magnetic order is ferrimagnetic in copper spinel, the A magnetic sublattice is aligned antiparallel with the B magnetic sublattice. The magnetic moment per molecule is about 1 μ_B/molecule (8 μ_B/f.u.) [6]. These properties are characteristic for the copper spinel synthesized by the classical ceramic route. For example, an increasing of the magnetic moment of the copper spinel at 2.3 μ_B/molecule (18.4 μ_B/f.u.) was reported for the copper spinel synthesized by rapid quenching [1,7]. The increase of the magnetization is associated with the redistribution of the cations between the crystallographic A and B sites. Thus, if one Cu^{2+} cation on the octahedral sites is exchanged with one Fe^{3+} cations from the tetrahedral sites a double magnetization is obtained compared with the inverse copper spinel. In the last two decades many studies have been dedicated to the synthesis of the copper ferrite in nanocrystalline/nanostructured state. The syntheses in nanocrystalline/nanostructured state improve/change the magnetic properties of the material. Among these techniques we mention: ball milling [4,8,11], co-precipitation [12,13], combustion route [14,15], etc. Ball milling technique is

* Corresponding author. Tel.: +40 264 401705; fax: +40 264 415054.
E-mail address: Ionel.Chicinas@stm.utcluj.ro (I. Chicinaş).

0272-8842/$36.00
doi:10.1016/j.ceramint.2011.10.026

one of the most versatile used to produce the nanostructured/nanocrystalline material. In order to obtain copper ferrite in nanostructured/nanocrystalline state using ball milling usually a polycrystalline copper ferrite is milled in order to reduce to crystallite and particle size [7]. Some combined routes are also used to synthesize copper ferrite such as co-precipitation followed by milling [16]. A high reversibility synthesis-decomposition was reported for the milling in the system Cu–Fe–O. Even at the beginning of the milling process $CuFe_2O_4$ or a stoichiometric mixture of CuO and α-Fe_2O_3 is used as starting material, during milling the formation and decomposition processes were noticed in both cases [17]. A mixed spinel structures, with Cu^{2+} cations distributed on both tetrahedral and octahedral sites, and also a superparamagnetic behavior were reported [11].

In this paper we present the synthesis of the nanocrystalline copper spinel ferrite using a route which combines reactive milling, heat treatment and mechanical milling. Some of the structural and magnetic properties of the synthesized powder are also presented and discussed.

2. Experimental details

A stoichiometric mixture of high purity commercial oxides powders (Alpha Aesar), copper oxide (CuO – tenorite) and iron oxide (α-Fe_2O_3 – hematite) was used as starting sample for the reactive milling. The milling conditions are similar with that described in the following reference [18]. The reader is referred to this reference for more details on the milling process. After this milling, in order to obtain single phase copper spinel several heat treatments in air have been tried, in temperature ranging from 600 to 1000° C.

After the synthesis of copper spinel ferrite as unique phase another milling process was applied in order to refine the crystallite size of the $CuFe_2O_4$. The second milling process was performed using the same mill and the same vial and disc rotational speeds (ω), respectively (Ω). In this case, agate balls and vial were used and the ball to powder ratio (BPR) was 11:1.

The formation of copper ferrite by reactive milling and heat treatment and its structural evolution in the second milling process was investigated by X-ray diffraction (XRD). A Siemens D5000 diffractometer which operates in reflection with CoK radiation (λ = 1.7903 Å) was used and the diffraction patterns were recorded in angular range 2θ = 15–90°. The mean crystallite size was calculated using Williamson–Hall's formula [19] and lattice parameter was determined using Celref 3 program [20]. For the fit and deconvolution of the diffraction patterns Fullprof program has been used [21].

The particle morphology and chemical homogeneity were investigated by scanning electron microscopy and X-ray microanalysis, using a Jeol-JSM 5600 LV scanning electron microscope equipped with an EDX spectrometer (Oxford Instruments, Inca 200 soft).

The magnetization versus field M(H) curves, were recorded at 300 K using the extraction sample method in a continuous magnetic field up to 8 T [22]. The spontaneous magnetization values have been derived from the extrapolation to zero field of the magnetization obtained in magnetic field higher than 5.5 T.

3. Results and discussion

The XRD patterns recorded for the as-milled (for 4, 8, 12, 16, 20, 24 and 30 h) on the oxides mixture and for the starting sample (ss) are presented in Fig. 1. In the X-ray diffraction pattern of the starting sample the Bragg reflections corresponding to the copper oxide – tenorite (CuO) and iron oxide – hematite (α-Fe_2O_3) are observed. For the 4 h milled sample a decreasing of the α-Fe_2O_3 peaks intensities together with a broadening of those peaks, as results of the crystallite size reduction and internal stresses induced by milling process are noticed. For this milling time, the disappearance of the Bragg reflections corresponding to the copper oxide phase can be noticed, together with the appearance of a new maxima. The disappearance of the CuO diffraction peaks is caused by the diffusion of the atoms of this phase into the α-Fe_2O_3 structure and the formation of a solid solution of CuO–Fe_2O_3, based on hematite structure, as has been reported previously [23]. The new peak, which is noticed, corresponds to the newly formed phase $CuFe_2O_4$ with cubic spinel structure – cuprospinel. This peak, (2 2 0), is not the most intense of the spinel structure (its relative intensity is about 30%). The most intense peak of the spinel structure, (3 1 1), it overlaps with the (1 1 0) diffraction maxima of the CuO–Fe_2O_3 solid solution. Therefore the most intense maxima of the formed solid solution seems to be the (1 1 0) maxima instead of the (1 0 4) maxima which is the most intense maxima of hematite, according to JCPDS reference file #33-0664. This indicates that, the amount of copper spinel which formed is significant. By increasing the milling time at 8 h, besides the peaks observed for the 4 h milled sample, a new Bragg reflection is observed at $2\theta = 42.6°$ in the diffraction patterns. This reflection is corresponding to a new phase which is formed in material at this milling time, Cu_2O – cuprite. This peak is the most intense peak of this phase and it appears as a

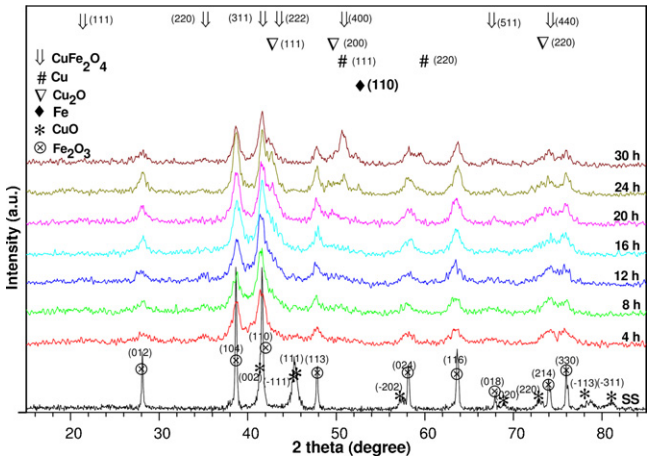

Fig. 1. X-ray diffraction patterns of the starting sample – ss (CuO + α-Fe_2O_3), and of the as-milled samples (for 4, 8, 12, 16, 20, 24 and 30 h of milling). The position of the diffraction peaks of each phase present in material is indicated at the top of the figure. For clarity, the diffraction patterns where vertically shifted.

shoulder over the (1 1 0) peak of the hematite. For the 12 and 16 h milled samples the same diffraction maxima and the same phases are present as for the 8 h milled sample. After 20 h of milling, a second peak, (2 0 0), corresponding to the Cu_2O is observed. This indicates an increasing of the cuprite amount in the material. This phase is formed by the decomposition of the α-Fe_2O_3–CuO solid solution and/or $CuFe_2O_4$, because in these non-equilibrium conditions, the formation of Cu_2O phase is probably more easily compared with the formation of CuO. For this time of milling (20 h) the presence of the elemental iron in the material is noticeable: the most intense peak, (1 1 0), of this phase can be observed in the diffraction pattern. The presence of iron in the obtained material is attributed to the powder contamination during milling [18]. Further milling, 24 and 30 h, leads to the dissociation of copper from oxides. The (1 1 1) and (2 2 0) diffraction lines of copper are present in the diffraction patterns. The amount of copper in the material increases by increasing the milling time from 24 to 30 h. The diffraction peaks of copper for the 30 h milled sample are more intense compared with the same peaks for the 24 h milled sample. The appearance of elemental copper by milling in the system Cu–Fe–O was also reported by Goya et al. and was explained by reduction of CuO [7]. In our experiments, the X-ray diffraction pattern shows that after 20 h of milling the Cu maxima increase and the Cu_2O maxima decrease. The elemental Cu is formed by reduction of Cu_2O. The formation of Cu_2O and Cu phases (both exhibiting a Me:O ratio very different from the starting ratio of 3:4) in the samples suggest some modifications in the spinel structure and also in CuO–Fe_2O_3 solid solution. Following the proposition of Ref. [7] it is possible that the spinel structure is not a simple copper spinel at longer milling times: the copper spinel was transformed in a mixed Cu–Fe spinel ($Cu_{1-x}Fe_{2+x}O_4$) during milling or in a mixture of $Cu_{1-x}Fe_{2+x}O_4$ and Fe_3O_4 (magnetite). Another fact that should be taken into account is that during the solid state reactions induced in the samples during milling an amount of oxygen could be released. If the $CuFe_2O_4$ is partially transformed in Fe_3O_4 during milling the following reaction could occurs:

$$12CuFe_2O_4 \rightarrow 8Fe_3O_4 + 6Cu_2O + 5O_2 \quad (1)$$

The resulting oxygen could be partially consumed at the transformation of the Fe_3O_4 in γ-Fe_2O_3 (maghemite) [24], which is an allotropic form of this:

$$2Fe_3O_4 + 1/2O_2 \rightarrow 3Fe_2O_3 \quad (2)$$

The reduction of the Cu_2O could naturally lead at the appearance of the copper in material:

$$Cu_2O \rightarrow 2Cu + 1/2O_2 \quad (3)$$

This last reaction is suggested by the decreasing of the areas ratio of the (1 1 1) peak of the cuprite and (1 1 0) peak of the solid solution (overlapping with (3 1 1) spinel peak). For the 20 h milled sample, the copper maxima is not yet identified in diffraction pattern, the area ratio is 0.71, whereas after 24 and 30 h of milling it is decreasing at 0.65 and 0.42 respectively. So, after 30 h of milling, a mixture of phases is present in the material. During milling these phases are forming: α-Fe_2O_3–CuO solid solution, Cu_2O, Cu, Fe and a mixture of copper spinels. These results confirmed once again the difficulty of the formation of the copper spinel – $CuFe_2O_4$ by milling starting from a stoichiometric mixture of oxides, as was reported in literature [17].

In order to synthesize the spinel copper ferrite, the samples with higher disorder degree, 30 h milled sample, was subjected to an heat treatment in vacuum or in air. Due to the oxygen contribution, the best results were achieved for the heat treatment in air. In Fig. 2 are presented the diffraction patterns recorded for the 30 h as-milled sample, 30 h milled and subsequently heat treated at 600, 800 and 1000 °C for 6 h samples. For the sample heat treated at 600 °C the copper spinel is the major phase in the material, also in the diffraction pattern are present the peaks corresponding to the hematite and tenorite as a result probably of the iron and copper oxidizing processes. By increasing the temperature of the heat treatment at 800 °C, the phases present in the material are copper spinel and hematite, the CuO reacts during this heat treatment. The heat treatment at 1000 °C for 6 h leads to a single phase material (in the limit of sensitivity of XRD technique); the phases resulted from milling process react entirely forming $CuFe_2O_4$ with spinel structure. Bearing in mind, that reactive milling induces a contamination of the powder with elemental Fe, the copper spinel obtained after heat treatment has an excess of Fe cations. In our spinel the ratio between Fe and Cu cations is consequently $1:(2+\gamma)$, instead of the starting 1:2 ratio where γ represents the amount of iron coming from the milling induced contamination. In this condition the chemical formula for our spinel in order to respect the stoichiometry corresponding to the metal/oxygen (3:4) as the product can be rewritten as: $Cu_1Fe_{2+\gamma}O_{4+1.33\gamma}$.

The copper spinel obtained after 30 h of milling and heat treatment at 1000 °C for 6 h was subjected to another milling process in order to obtain a nanocrystalline/nanostructured structure. The XRD patterns for this copper ferrite milled 0, 1,

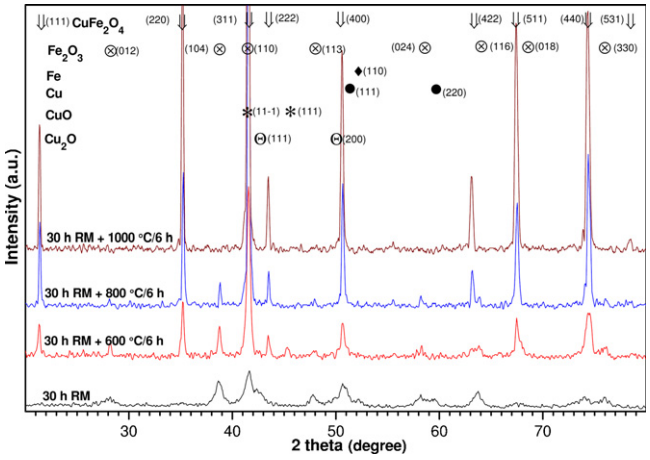

Fig. 2. X-ray diffraction patterns of the 30 h as-milled sample (30 h RM in figure), 30 h milled samples and heat treated for 6 h at 600, 800 and 1000 °C. The position of the diffraction peak for each phase is indicated in the figure. For clarity, the diffraction patterns where vertically shifted.

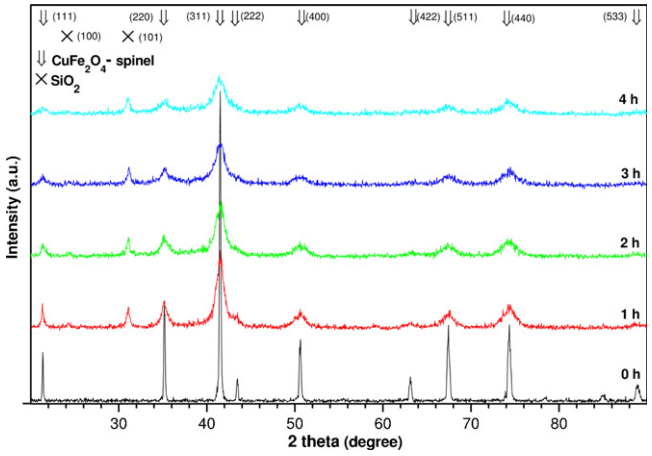

Fig. 3. X-ray diffraction patterns of the $CuFe_2O_4$ synthesized after 30 h of milling and heat treatment at 1000 °C and then milled 0, 1, 2, 3 and 4 h. The position of the diffraction peak for each phase is indicated in the figure. For clarity, the diffraction patterns where vertically shifted.

2, 3 and 4 h are presented in Fig. 3. After only 1 h of milling the peaks corresponding to the spinel phase are broadened, due to the crystallite size reduction. Also, at this time of milling, in the XRD patterns two new peaks can be observed. Those peaks are identified as (1 0 0) and (1 0 1) of the SiO_2 – agate, so the copper ferrite is contaminated during milling. The amount of the agate contamination was estimate at 8 up to 10% by areas ratio.

For the other milling time (2, 3 and 4 h) the same phases seems to be present in the material. But, at a closer analysis of the diffractions patterns, for the 4 h milled sample the diffraction maxima of hematite can be remarked. The corresponding fit of the X-ray diffraction pattern and its deconvolution are presented in Fig. 4b. Similar study shows that for the 2 and 3 h milled sample the hematite is already present in the material. This is formed during milling as results of the decomposition of the copper spinel with Fe cations excess. This is in very good agreement with the earlier reported results, confirming once again the reversibility in the Fe–Cu–O system [17]. The amount of hematite which was formed by spinel decomposition was estimated using the areas ratio at 7 up to 9%. The amount of the SiO_2 impurities for the milled sample remains at the same value for the entire period of milling, probably during milling a piece of agate was detached from the vial or balls in the early stage of milling. The fit and the deconvolution for the 1 h milled sample is presented in Fig. 4a and for this milling time there is no evidence of the copper spinel decomposition. The diffraction pattern shows only the peaks corresponding to the copper spinel ferrite and the agate impurities. One cannot exclude to have an incipient decomposition, a small amount of hematite formed at this milling time, we have checked this possibility, but this is not detectable by X-ray diffraction technique.

The mean crystallite size of the $CuFe_2O_4$ phase is strongly reduced by milling process. If the mean crystallite size of the un-milled copper ferrite (as-obtained after heat treatment, referred to as "0 h" in the figure), is about 250 nm, 1 h of milling leads to a reduction down to 9 nm. Further increasing of

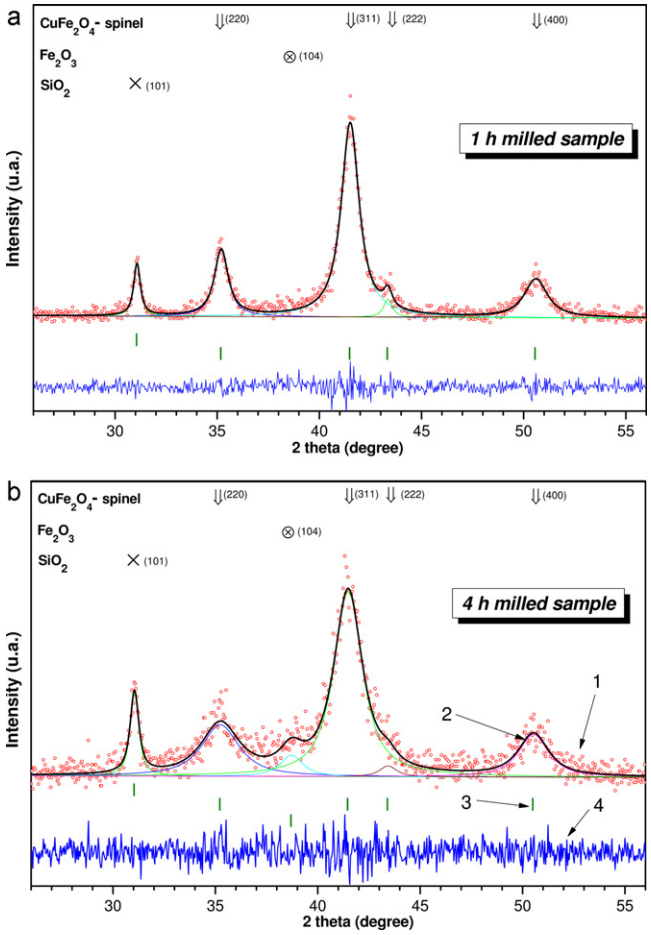

Fig. 4. Fit and deconvolution of the XRD patterns including the following Bragg peak contribution the hematite (1 0 4), agate (1 0 1) and copper ferrite (2 2 0), (3 1 1), (2 2 2) and (4 0 0) for the 1 h milled sample (a) and the 4 h milled sample (b). (1) Experimental XRD points; (2) the best fit curve of the XRD experimental points; (3) peaks position and (4) difference between the experimental points and the corresponding fit. The corresponding diffraction lines are marked for each phase in the top part of the figures.

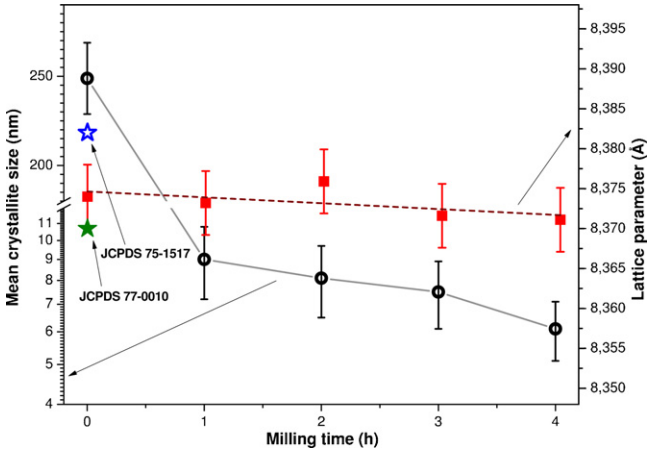

Fig. 5. Evolution of the mean crystallite size and of the lattice parameter of the $CuFe_2O_4$ spinel versus milling time. For the reference the values of the lattice parameter are given from the files JCPDS 77-0010 and JCPDS 75-1517.

the milling time leads to a refinement of the crystallite size. After 4 h of milling, the crystallite size decreased at about 6 nm. The evolution of the mean crystallite size as a function of the milling time for the $CuFe_2O_4$ is presented in Fig. 5 along side the evolution of the lattice parameter versus milling time. For the reference the values of the lattice parameter from the JCPDS 77-0010 and JCPDS 75-1517 files are given. The lattice parameter determined for the un-milled (0 h) $CuFe_2O_4$ is 8.374 Å. This value of the lattice parameter is closer to the values: 8.370 Å (JCPDS 77-0010) corresponding to the inverse spinel structure $(Fe^{3+})^A(Cu^{2+}Fe^{3+})^BO_4$, according to Verwey and Heilmann [25] and 8.382 Å (JCPDS 75-1517) which correspond to a partially inverse spinel and with an excess of iron cations $(Cu_{0.21}{}^{2+}Fe_{0.79}{}^{3+})^A(Cu_{0.705}{}^{2+}Fe_{1.295}{}^{3+})^BO_4$. A larger lattice parameter for the obtained copper ferrite suggests the presence of the Cu^{2+} cations in tetrahedral spinel structure sites. The presence of Cu^{2+} cations in tetrahedral sites leads to the distortion of the tetragon in the spinel due to their higher ionic radius, 0.72 Å, compared with the 0.67 Å Fe^{3+} cation radius. The milling process does not modify substantially the value of the lattice parameter, but the trend is decreasing. This slight decreasing suggests a partial reordering of the cations in the copper ferrite. For the milled sample (1–4 h) the lattice parameter is between 8.371 and 8.376 Å. The value of the lattice parameter after 4 h of milling is 8.371 Å, a value very close of the one for the total inverse spinel structure.

In Fig. 6 are presented the magnetization curves recorded at room temperature for the $CuFe_2O_4$ samples milled 0, 1, 2, 3 and 4 h. For the un-milled sample, the magnetization saturated relatively easily (at small external magnetic field). In the mean time, for the milled samples a lack of saturation can be remarked, even if the applied magnetic field reaches 8 T. This behavior is associated with the canted effect of the spins at the surface of the particles induced by the milling process and also with the superparamagnetism [11]. The superparamagnetism is induced by the very fine particles of copper ferrite which results from the milling process [18].

The spontaneous magnetization of the $CuFe_2O_4$ decreases upon increasing the milling time. In Fig. 7 is presented the

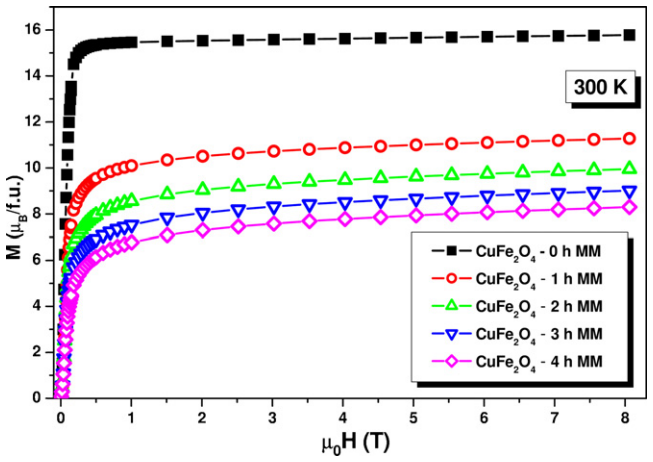

Fig. 6. Room temperature magnetization curves recorded for the $CuFe_2O_4$ samples milled 0, 1, 2, 3 and 4 h.

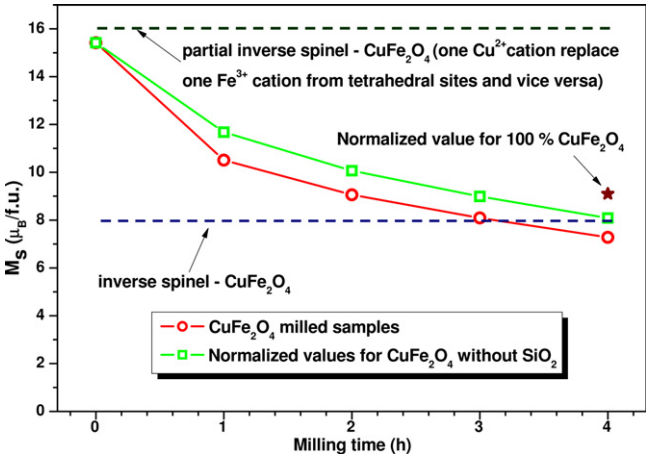

Fig. 7. Spontaneous magnetization of the $CuFe_2O_4$ milled 0, 1, 2, 3 and 4 h. For comparison are given two values corresponding to the $CuFe_2O_4$ inverse spinel and $CuFe_2O_4$ partial inverse spinel (one Cu^{2+} cation replace one Fe^{3+} cation from tetrahedral sites and vice versa) structures.

evolution of the spontaneous magnetization for the copper ferrite milled between 0 and 4 h as a function of milling time. For comparison, in the same figure are given the values for the spontaneous magnetization calculated for the $CuFe_2O_4$ with totally inverse and with partially inverse (one Cu^{2+} cation replace one Fe^{3+} cation from tetrahedral sites and vice versa) spinel structures, 16 μ_B/f.u. (2 μ_B/molecule) and 8 μ_B/f.u. (1 μ_B/molecule) respectively. The spontaneous magnetization for the milled samples normalized, considering the amount of agate as being null, are shown in Fig. 7. For the 4 h milled sample, which contains a small amount of hematite besides the SiO_2 contamination, the value of spontaneous magnetization normalized at 100% of $CuFe_2O_4$ is also shown in Fig. 7. The spontaneous magnetization obtained for the un-milled copper ferrite is very closed to the value calculated for the partially inverse spinel structure where, one Cu^{2+} cation replace one Fe^{3+} cation from tetrahedral sites and vice versa. This indicate that the copper ferrite formed by milling and heat treatment has a partial inverse spinel structure, where the Cu^{2+} and Fe^{3+} cations are both distributed between the A and B sites. The formula of the copper ferrite considering the cations distribution and the iron contamination becomes: $(Cu_{1-\delta}Fe_\delta)^A(Fe_{2+\gamma-\delta}Cu_\delta)^BO_{4+1.33\gamma}$, where δ represent the degree of inversion of the cations between A and B sites. The value of the spontaneous magnetization for the un-milled copper spinel ferrite (0 h) is 15.42 μ_B/f.u. (1.93 μ_B/molecule) and decreases at 7.28 μ_B/f.u. (0.91 μ_B/molecule) after 4 h of milling. This reduction of the spontaneous magnetization can be due to (i) the canted magnetic moments at the surface of the particles (spin canted effect) and (ii) to the cations partial redistribution between tetrahedral and octahedral sites during milling [11,26]. Another factor which can contribute to the spontaneous magnetization reduction is the structural defects/structural disorder induced by milling process. After 3 h of milling the magnetization is almost at the same value as one calculated for the copper spinel with totally inverse structure. Increasing the milling time the spontaneous magnetization decreases at a value that is lower compared with the copper ferrite with inverse spinel. The reduced magnetization for the copper

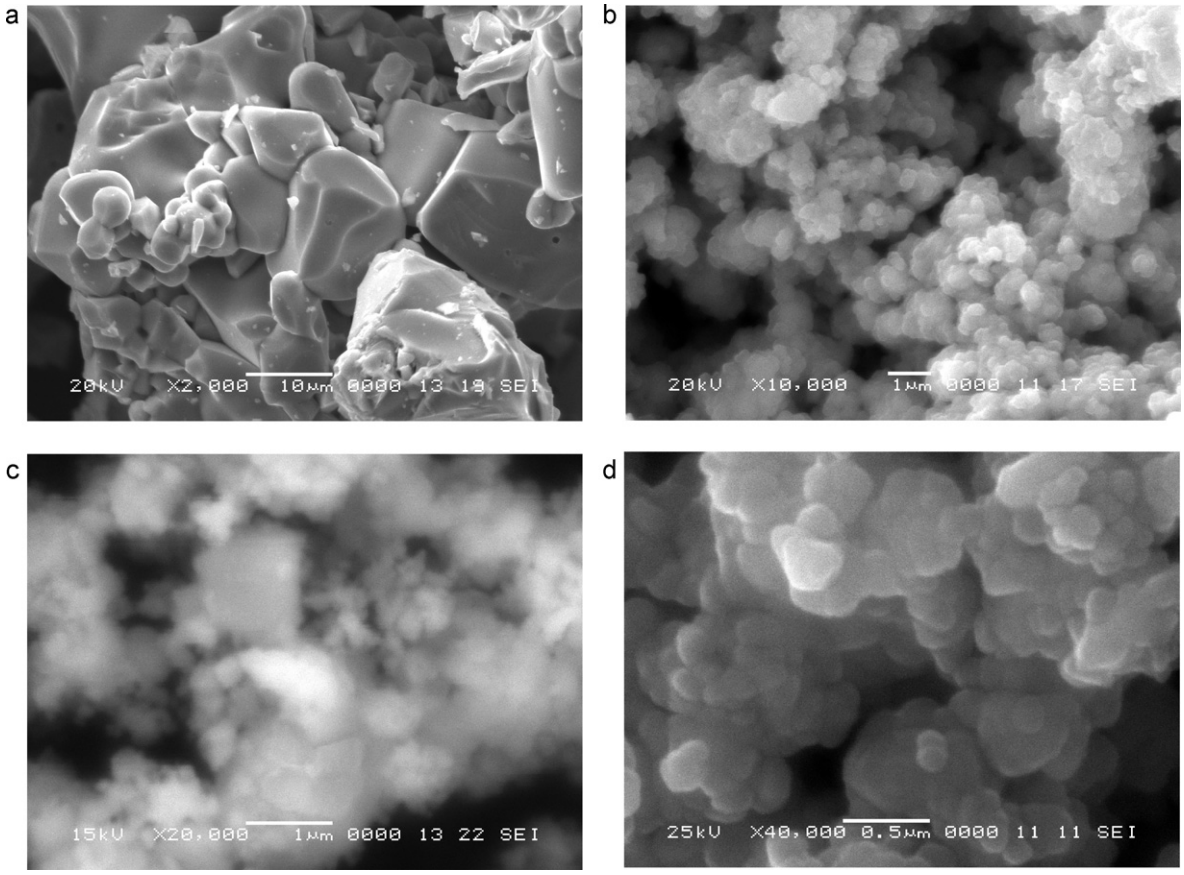

Fig. 8. SEM micrographs of the samples: (a) $CuFe_2O_4$ synthesized after 30 h of reactive milling and subsequent heat treatment at 1000° for 6 h at 2000×, (b), (c) and (d) for the nanocrystalline $CuFe_2O_4$ obtained after 1 h of mechanical milling at 10,000×, 20,000× and respectively 40,000×.

spinel milled samples is partially caused by the contamination of the powder with agate. For example for the 4 h milled sample the normalized value for spontaneous magnetization of the $CuFe_2O_4$ without SiO_2 is 8.09 μ_B/f.u. This value is almost the same as the one calculated for the inverse spinel copper ferrite. But, taking in account the copper ferrite decomposition, revealed with the XRD, the spontaneous magnetization of the copper spinel can be higher that the experimental value. Considering an amount of hematite of 10%, by normalizing at 100% of copper spinel (at room temperature the hematite is antiferromagnetic) a 9.1 μ_B/f.u. (1.14 μ_B/molecule) was obtained. This spontaneous magnetization value is greater compared with the magnetization calculated for the totally inverse copper spinel and suggest that the milled samples have a partially inverse spinel structure. In 4 h of milling the spontaneous magnetization is reduced at 60% for the copper ferrite.

Assuming that the magnetic moments are aligned parallel in each magnetic sublattice and the A and B magnetic sublattices are oriented antiparallel [6], the degree of inversion (δ) for the copper spinel was calculated for all the milling time, without taking into account the iron contamination. For the un-milled sample a degree of inversion $\delta = 0.116$ was determined. In this condition the spinel has the following formula: $(Cu_{0.116}Fe_{0.884})^A(Fe_{1.116}Cu_{0.884})^BO_4$. The degree of inversion is close the degree of inversion calculated for one Cu^{2+} cation in tetrahedral sites for each unit cell, $\delta = 0.125$. The degree of inversion for the 1 h milled sample decreases at $\delta = 0.074$. After 4 h of milling, the degree of inversion calculated for the saturation magnetization normalized at 100% copper ferrite reaches $\delta = 0.020$. Actually, the degree of inversion could be higher for each milling time considering that the calculations were done for the saturation magnetization at 300 K. Goya et al. reported a saturation magnetization of the milled spinel copper ferrite lower about 10% at 300 K compared with the 4.2 K measurement [7]. These facts suggest also a redistribution of the cations during milling in the spinel structure.

Fig. 8 shows the SEM micrographs obtained for the $CuFe_2O_4$ synthesized by 30 h of reactive milling and subsequent heat treated at 1000° for 6 h and for the nanocrystalline $CuFe_2O_4$ obtained after 1 h of mechanical milling. For the $CuFe_2O_4$ sample in polycrystalline state the particles have dimensions which vary from 0.3 to 0.5 at tens of microns and the particles shape is irregular (Fig. 8a). After 1 h of mechanical milling the particles dimensions are drastically reduced (Fig. 8b–d). From the analysis of the SEM micrographs one can estimate that the largest dimensions for the particles is about 1–2 μm. Alongside of those micrometric particles coexists small particles of tens and hundreds of nanometers, nanosized particles. Those particles are agglomerated. The smaller particles seems to have about 30–50 nm, but those particles are actually smaller due to the fact that before SEM analysis the samples were covered with an Au layer of 2.5 nm

thickness to avoid electrical charge. On the other hand due to the fact that particles are agglomerated even slightly smaller particles could be present in the sample. These small particle sizes could be at the origin of superparamagnetic contribution.

4. Conclusions

By reactive milling of a stoichiometric mixture of CuO and α-Fe_2O_3 a mixture between a solid solution of those oxides and a cubic spinel phase was obtained after 4 h of milling. Continuing the milling process, a mixture of copper oxides is formed, in addition, a contamination of the sample with Fe is noticed. For milling time higher that 20 h a dissociation Cu is remarked, probably due to the reduction of copper oxide (Cu_2O). The single cubic copper spinel phase was achieved by subsequent heat treatment applied to the 30 h milled sample. The structure of the synthesized spinel phase is partially inversed and has a higher magnetic moment compared with the calculated one for the total inverse spinel. The obtained copper ferrite was subjected to a second milling. The crystallite size is reduced at 9 nm after only 1 h of milling. The magnetization of the milled samples is reduced compared with the un-milled copper ferrite due to the partial redistribution of the cations during milling in the structure, structural defects/structural disorder and spin canted effect. For the copper ferrite milled more that 1 h a decomposition of copper ferrite and forming the hematite phase was observed. For the nanocrystalline samples a lack of saturation of the magnetization can be due to the spins canted and probably to the very fine particles which are superparamagnetic.

Acknowledgment

This work was supported by CNCSIS – UEFISCSU, project number PNII – IDEI code 1519/2008.

References

[1] A. Goldman, Modern Ferrite Technology, Second edition, Springer, Pittsburgh, 2006.
[2] J. Ding, P.G. McCormick, R. Street, Formation of spinel Mn–ferrite during mechanical alloying, J. Magn. Magn. Mater. 171 (1997) 309–314.
[3] M.I. Rosales, M.P. Cuautle, V.M. Castaño, Microstructure and magnetic properties of Ni–Zn ferrites, J. Mater. Sci. 33 (1998) 3665–3669.
[4] S.J. Stewart, R.C. Mercader, R.E. Vandenberghe, G. Cernicchiaro, R.B. Scorzelli, Magnetic anomalies and canting effects in nanocrystalline spinel copper ferrites $Cu_xFe_{3-x}O_4$, J. Appl. Phys. 97 (2005), 054304.
[5] B.S. Randhawa, H.S. Dosanjh, M. Kaur, Preparation of spinel ferrites from citrate precursor route – a comparative study, Ceram. Int. 35 (2009) 1045–1049.
[6] B.D. Cullity, C.D. Graham, Introduction to Magnetic Materials, 2nd ed., IEEE Press & Wiley, New Jersey, 2009.
[7] G.F. Goya, H.R. Rechenberg, J.Z. Jiang, Structural and magnetic properties of ball milled copper ferrite, J. Appl. Phys. 84 (2) (1998) 1101–1108.
[8] D. Prabhu, A. Narayanasamy, K. Shinoda, B. Jeyadeven, J.-M. Greneche, K. Chattopadhyay, Grain size effect on the phase transformation temperature of nanostructured $CuFe_2O_4$, J. Appl. Phys. 109 (2011) 013532.
[9] S. Kameoka, T. Tanabe, A.P. Tsai, Spinel $CuFe_2O_4$: a precursor for copper catalyst with high thermal stability and activity, Catal. Lett. 100 (1–2) (2005) 89–93.
[10] J.E. Tasca, C.E. Quincoces, A. Lavat, A.M. Alvarez, M.G. González, Preparation and characterization of $CuFe_2O_4$ bulk catalysts, Ceram. Int. 37 (2011) 803–812.
[11] J.Z. Jiang, G.F. Goya, H.R. Rechenberg, Magnetic properties of nanostructured $CuFe_2O_4$, J. Phys.: Condens. Matter 11 (1999) 4063–4078.
[12] J.A. Gomes, M.H. Sousa, F.A. Tourinho, J. Mestnik-Filho, R. Itri, J. Depeyrot, Rietveld structure refinement of the cation distribution in ferrite fine particles studied by X-ray powder diffraction, J. Magn. Magn. Mater. 289 (2005) 184–187.
[13] M. Siddique, N.M. Butt, Effect of particle size on degree of inversion in ferrites investigated by Mössbauer spectroscopy, Physica B 405 (2010) 4211–4215.
[14] N.M. Deraz, Size and crystallinity-dependent magnetic properties of copper ferrite nano-particles, J. Alloys Compd. 501 (2010) 317–325.
[15] V. Krishnan, R.K. Selvan, C.O. Augustin, A. Gedanken, H. Bertagnolli, EXAFS and XANES investigations of $CuFe_2O_4$ nanoparticles and $CuFe_2O_4$–MO_2 (M = Sn, Ce) nanocomposites, J. Phys. Chem. C 111 (2007) 16724–16733.
[16] E. Manova, T. Tsoncheva, D. Paneva, M. Popova, N. Velinov, B. Kunev, K. Tenchev, I. Mitov, Nanosized copper ferrite materials: mechanochemical synthesis and characterization, J. Solid State Chem. 184 (2011) 1153–1158.
[17] G.F. Goya, H.R. Rechenberg, Reversibility of the synthesis–decomposition reaction in the ball-milled Cu–Fe–O system, J. Phys.: Condens. Matter 10 (1998) 11829–11840.
[18] T.F. Marinca, I. Chicinaş, O. Isnard, V. Pop, F. Popa, Synthesis, structural and magnetic characterization of nanocrystalline nickel ferrite – $NiFe_2O_4$ obtained by reactive milling, J. Alloys Compd. 509 (2011) 7931–7936.
[19] G.K. Williamson, W.H. Hall, X-ray line broadening from filed aluminium and wolfram, Acta Metall. 1 (1953) 22–31.
[20] J. Laugier, B. Bochu, CELREF V3. Developed at the Laboratoire des Materiaux et du Genie Physique, Ecole Nationale Superieure de Physique de Grenoble (INPG) (2003) http://www.inpg.fr/LMGP.
[21] J. Rodriquez-Carvajal, Recent advances in magnetic structure determination by neutron powder diffraction, Physica B 192 (1993) 55–69.
[22] A. Barlet, J.C. Genna, P. Lethuillier, Insert for regulating temperatures between 2 and 1000 K in a liquid helium dewar. Description and cryogenic analysis, Cryogenics 31 (1991) 801–805.
[23] J.S. Jiang, X.L. Yang, L. Gao, J.K. Guo, Nanostructured CuO–α-Fe_2O_3 solid solution obtained by high-energy ball milling, Mater. Sci. Eng. A 392 (2005) 179–183.
[24] K. Haneda, A.H. Morrish, Magnetite to maghemite transformation in ultrafine particles, J. Phys. 4 (1977) C1321–C1323.
[25] E.J.W. Verwey, E.L. Heilmann, Physical properties and cation arrangement of oxides with spinel structures. 1. Cation arrangement in spinels, J. Chem. Phys. 15 (4) (1947) 174–180.
[26] S.J. Stewart, M.J. Tueros, G. Cernicchiaro, R.B. Scorzelli, Magnetic size growth in nanocrystalline copper ferrite, Solid State Commun. 129 (2004) 347–351.